21

Modelling of the effective dielectric constant of aluminum oxyhydroxides porous 3D nanostructures in the THz range

© A.V. Andreev[1], E.A. Kekkonen[2], A.A. Konovko[1], A.N. Khodan[3]¶

[1] Lomonosov Moscow State University, Faculty of Physics, Moscow, Russia
[2] GBOU School № 1547, Moscow, Russia
[3] Frumkin Institute of Physical Chemistry and Electrochemistry of the Russian Academy of Sciences (IPCE RAS), Moscow, Russia[

¶e-mail: anatole.khodan@gmail.com

Received September 01, 2025
Revised December 19, 2025
Accepted December 19, 2026

The article is devoted to quantitative assessments of the complex dielectric constant of highly porous media, the structure of which is a 3D network of aluminium oxyhydroxides nanofibrils (PMOA). Based on the Bruggeman formula and using the Maxwell−Garnett approximation, an effective medium model has been developed that allows us to take into account the depolarization effects in PMOA materials caused by the elongated elliptical shape of the fibrils. Quantitative estimates of the dielectric constant and refractive index were made on the basis of model approximations taking into account changes in the structural and phase state of PMOA nanomaterials upon annealing in the temperature range of 20−1650°C. The possibility of assessing dielectric properties and optical anisotropy is shown taking into account the presence of texture associated with the features of 1D growth of nanofibrils and the process of formation of the general monolithic porous 3D nanostructure of PMOA materials.

Keywords: nanomaterials, mesoporous materials, aluminium oxyhydroxides, nanofibrils, 3D structure, dielectric constant.

DOI: 10.61011/0000000000

Introduction

The development of methods for the synthesis of three-dimensional nanostructures with specified physical and chemical properties underlies the creation of new nanomaterials and nanocomposites, the functional properties of which allow solving various applied problems in the field of heterogeneous photocatalysis and photosynthesis [1], photocatalytic biodegradation of microorganisms [2], to create optics elements based on them for the IR and THz range [3], antenna arrays, photonic crystals and metamaterials. The physical properties of materials based on monolithic highly porous 3D nanostructures consisting of a network of aluminum hydroxide nanofibrils (AHPM) can vary widely depending on the methods of chemical or thermal treatment [4,5]. During annealing in the 25−1700° C temperature range, the overall porous 3D nanostructure of the AHPM materials is preserved, but the linear dimensions of the samples are isotropically reduced to ~ 10 times, the morphology of the nanofibrils changes significantly — the average diameter increases from ~ 4.8 to 300 nm, the chemical and phase compositions change from amorphous hydrated pseudobemite $Al_2O_3 \cdot 4.6H_2O$ to crystalline oxides: γ-, θ- and α-Al_2O_3. Physical properties can vary within the following limits: bulk density — from ~ 0.02 to 3 g/cm^3, open porosity — from 99.6% to 25%, specific surface area decreases by more than 100 times: from ~ 300 to ~ 1 cm^2/g. Previously, a physical model was proposed that quantitatively describes the evolution of a porous 3D nanostructure of AHPM materials during annealing [4,5].

The choice of THz range optics materials that combine the required refractive index with low loss and scattering is currently quite limited. Porous 3D nanostructures and nanocomposites based on them open up prospects for the creation of new materials and optical media for the THz range. The controlled change of the refractive index in materials based on AHPM is possible either by reducing the total porosity and increasing the bulk density of the material during annealing (Fig. 1), or by impregnating the free volume of a porous 3D structure with metal or oxide nanoparticles in order to change/increase the overall effective refractive index in a given spectral range.

A necessary step in the development of new functional materials with specified optical properties is the creation of physical models that quantify their electrodynamic, optical and dispersion properties in various spectral ranges (infrared, terahertz, etc.). The results of detailed experimental studies of changes in the chemical composition of nanofibrils, their morphology, and 3D structure during annealing were quantified within the framework of a physical model of the evolution of AHPM materials, where a cube with an edge equal to „averaged“ length of the AHPM nanofibrill — filaments $Al_2O_3 \cdot nH_2O$ was adopted as the „lattice cell“. It has been shown that changes in the physico-chemical properties of AHPM are well described by a geometric factor: the aspect ratio length/diameter for the average size of nanofibrils [4]. Based on the results of experimental

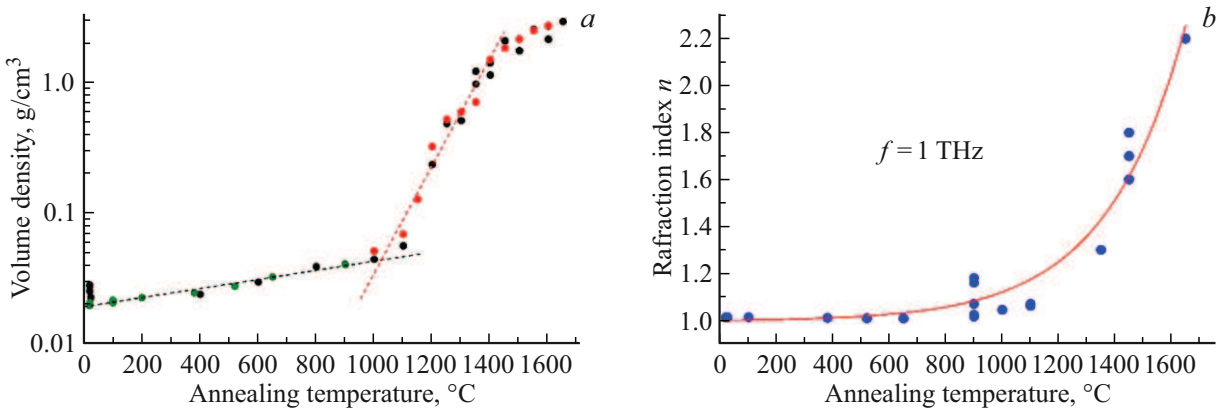


Figure 1. Physical properties of AHPM materials as a function of temperature of T],°C of isochronous annealing for 4 h: (a) volume density change; (b) dependence of the real part of the refractive index measured at a frequency of 1 THz.

studies and a physical model of the evolution of AHPM materials, we have proposed a model of the dielectric constant of 3D nanomaterials, which allows quantifying the influence of factors such as porosity, texture, structural water content, as well as their changes depending on the temperature and time of annealing of the material.

Model of dielectric permittivity of nanostructured aluminum hydroxide

The 3D structure in monolithic porous AHPM samples is formed by a network of intertwined fibrils of hydrated aluminum oxide, the average diameter of which ranges from 4 to 10 nm and the length is in the range of 150–300 nm. After annealing at a temperature of 1300°C, the fibrils shorten and thicken, their shape approaches an ellipsoid, while their maximum size decreases to 130–270 nm with an average value of ~ 200 nm. An estimate of the diameter of the fibrils based on their specific surface area gives a value of 183 nm. It follows from this that the AHPM samples are sufficiently homogeneous for wavelengths $\lambda > 3\,\mu$m, and their optical properties can be described by the effective dielectric constant [6]. The total composition of AHPM depends on the annealing temperature and varies from $Al_2O_3 \cdot nH_2O$, where $n = 3.6–4.3$ is in the initial state at 25°C, to the well-crystallized phase α-Al_2O_3 after annealing 4 h at 1300°C, which does not contain both structural and adsorbed water from the air. To build a model of the effective permittivity of the AHPM, it is necessary to specify the permittivity of the specified components [7–9]. Assuming the humidity of the air is zero, its dielectric constant is assumed to be $\varepsilon_{\text{air}} = 1$. The dielectric constant of fully dehydrated alumina $\varepsilon_{Al_2O_3}$) in the THz frequency range can be obtained by approximating experimental data taken from the article [4], by the following expressions:

$$\varepsilon' = \varepsilon'_\infty + \nu_{pl}^2 \frac{\nu_0^2 - \nu^2}{(\nu_0^2 - \nu^2)^2 + \nu^2\Gamma^2/(2\pi)^2},$$

$$\delta = \delta_1 + \delta_2 e^{q_2\nu}, \qquad \varepsilon_{Al_2O_3} = \varepsilon' + i\varepsilon'\delta, \tag{1}$$

where ε' is the real part of the dielectric constant, δ is the tangent of the loss angle, ν is the frequency of THz, and ε'_∞, ν_{pl}, ν_0, Γ, q_2, δ_1, δ_2 are the adjustment coefficients. In this case, the real part of the dielectric constant is modeled based on the well-known Lorentz function to match the Kramers–Kronig ratios, and for the tangent of the loss angle, which varies slowly in the specified frequency range, a formal expression is chosen that provides sufficient approximation accuracy.

Various numerical values of the dielectric constant of „free“ (volumetric) water are given in publications on water spectroscopy in the THz range. In our model, we used an expression from Ref. [6]:

$$\varepsilon_w = \varepsilon_\infty + \frac{\Delta\epsilon_{1s}}{1 + 2\pi i\tau_1\nu \cdot 10^{12}} + \frac{\Delta\epsilon_{2s}}{1 + 2\pi i\tau_{2s}\nu \cdot 10^{12}} + \frac{A}{\omega_0^2 - (2\pi\nu \cdot 10^{12})^2 + i\gamma_1 2\pi\nu \cdot 10^{12}}. \tag{2}$$

It should be noted that the parameters of the model depend on the temperature [10], and an adequate model of the dielectric constant of a medium including water should take this dependence into account. However, we assume in this paper that the temperature of the sample after annealing is fixed and equal to $T = 20$°C.

A similar formula [11] is proposed for the permittivity of structural (ε_{sw}) and absorbed (ε_{aw}) water in the THz frequency range, differing from the expression for „free“ water only by the value of the adjustment coefficients:

$$\varepsilon_{sw} = \varepsilon_{sw\infty} + \frac{\Delta\epsilon_{1s}}{1 + 2\pi i\tau_{1s}\nu \cdot 10^{12}} + \frac{\Delta\epsilon_{2s}}{1 + 2\pi i\tau_{2s}\nu \cdot 10^{12}} + \frac{A_s}{\omega_{0s}^2 - (2\pi\nu \cdot 10\nu^{12})^2 + i\gamma_{1s} 2\pi\nu \cdot 10^{12}}, \tag{3}$$

$$\varepsilon_{aw} = \varepsilon_{aw\infty} + \frac{\Delta\epsilon_{1a}}{1 + 2\pi i\tau_{1a}\nu \cdot 10^{12}} + \frac{\Delta\epsilon_{2a}}{1 + 2\pi i\tau_{2a}\nu \cdot 10^{12}} + \frac{A_a}{\omega_{0a}^2 - (2\pi\nu \cdot 10\nu^{12})^2 + i\gamma_{1a}2\pi\nu \cdot 10^{12}}, \quad (4)$$

The optical properties of a composite material, which includes particles with a complex structure, generally depend on how the substance is distributed, and therefore the field in these particles [12]. However, without having sufficiently precise information about the distribution of components in the fibrils, let us assume that absorbed water, structural water, and aluminum oxide are distributed isotropically in the volume of the fibrils on average. To more accurately account for the contribution of water of various types, we first calculate the effective permittivity of the medium „absorbed water in structural water" according to the effective medium model using the Bruggeman formula [13,14]:

$$(1-f)\frac{\varepsilon_{ew} - \varepsilon_{sw}}{\varepsilon_{sw} + 2\varepsilon_{ew}} + f\frac{\varepsilon_{ew} - \varepsilon_{aw}}{\varepsilon_{aw} + 2\varepsilon_{ew}} = 0. \quad (5)$$

Here, ε_{sw}, ε_{aw} and ε_{ew} are the dielectric permittivities of structural water, absorbed water and their mixtures, respectively, f is the volume fraction of absorbed water, $1-f$ is the volume fraction of structural water. The choice of the model is due to the fact that in the formula (5) both components of the medium enter symmetrically, and the interaction of the particle with other particles is taken into account in the approximation of the averaged field. Solving the equation (5) with respect to ε_{ew}, we obtain the analytical expression

$$\varepsilon_{ew} = \frac{1}{4}\left(-\varepsilon_{aw} + 3f\varepsilon_{aw} + 2\varepsilon_{sw} - 3f\varepsilon_{sw} + \sqrt{(8\varepsilon_{aw}\varepsilon_{sw} + [\varepsilon_{aw}(3f-1) + \varepsilon_{sw}(2-3f)]^2}\right). \quad (6)$$

Taking into account the change in f and the volume fraction of aluminum oxide g with increasing annealing temperature according to the model of the evolution of the structure [4], the dielectric constant ε_{fib} of the composite fibrillation material is found similarly by considering a two-component medium formed by aluminum oxide with a dielectric constant of $\varepsilon_{Al_2O_3}$ and water with an effective dielectric constant ε_{ew}:

$$\varepsilon_{\text{fib}} = \frac{1}{4}\left(-\varepsilon_{Al_2O_3} + 3g\varepsilon_{Al_2O_3} + 2\varepsilon_{ew} - 3g\varepsilon_{ew} + \sqrt{8\varepsilon_{Al_2O_3}\varepsilon_{ew} + [\varepsilon_{Al_2O_3}(3g-1) + \varepsilon_{ew}(2-3g)]^2}\right). \quad (7)$$

The influence of the shape of aluminum oxide fibrils on the dielectric constant of AHPM is manifested in the anisotropy of the polarizability of both individual fibrils and the material as a whole. A model of the AHPM unit cell was proposed in Ref. [4], in which, for simplicity of estimates, the fibrillation is considered a straight circular cylinder. However, the fibrils are devoid of flat bases, the diameter of the fibrill can vary along its axis, and upon annealing, the fibrils acquire an ellipsoidal shape. Therefore, we will assume that the fibrils have the shape of elongated ellipsoids. We find the dielectric constant of the AHPM using the Maxwell-Garnett relation for ellipsoidal particles in a homogeneous medium [14]. This approximation is acceptable far from plasmon resonance. The polarizabilities of such spheroids are given by the following expressions:

$$\alpha_x = \frac{ca^2}{3}\frac{\varepsilon_{\text{fib}} - \varepsilon_{\text{air}}}{\varepsilon_{\text{air}} + L_1[\varepsilon_{\text{fib}} - \varepsilon_{\text{air}}]}$$

$$\alpha_z = \frac{ca^2}{3}\frac{\varepsilon_{\text{fib}} - \varepsilon_{\text{air}}}{\varepsilon_{\text{air}} + L_0[\varepsilon_{\text{fib}} - \varepsilon_{\text{air}}]},$$

$$L_m = \frac{1}{1 - (\varepsilon_1^m/\varepsilon_{air}}, \quad (8)$$

$$L_0 = (\xi_0^2 - 1)\left(\frac{\xi_0}{2}\ln\left(\frac{\xi_0 + 1}{\xi_0 - 1}\right) - 1\right),$$

$$L_1 = \frac{1}{2}(1 - L_0) \qquad \xi_0^2 = \frac{\alpha^2}{\alpha^2 - 1}, \quad (9)$$

where $\varepsilon_{\text{air}} = 1$ is the dielectric constant of air, ξ is the volume fraction of fibrils in AHPM. In particular, if the fibrils have the shape of an ellipsoid of rotation and are elongated (textured) in the direction of AHPM growth (along the axis Z, in the perpendicular plane XY the fibrils are randomly oriented [4,5]), the aspect ratio approaches $\sim \alpha$, and the dimensionless depolarization factor takes the form

$$L = L_z = \frac{\alpha\arccos(\alpha)}{(\alpha^2 - 1)^{3/2}} - \frac{1}{\alpha^2 - 1}, \quad L_x = L_y = \frac{1 - L}{2}. \quad (10)$$

The geometric formfactor of a fibrillation is the ratio of length to diameter, according to Ref. [4,5], can be extracted from the following expressions for α_D (at annealing temperature $T < 1000^\circ$C) and α_B (at annealing temperature $T \geq 1000^\circ$C):

$$\alpha_D = \alpha_0\left(1 - \frac{1}{a_0}\sqrt{tD_0\exp\left(-\frac{E_D}{RT}\right)}\right)^{3/2}, \quad (11)$$

$$\alpha_B = \alpha_0\left(\frac{\rho_0}{\rho_f} + \exp\left(-tB_0\left(-\frac{E_b}{RT}\right)\right)\right)^{1.2}. \quad (12)$$

The designations from Ref. [4,5] are used here: initial length and diameter of fibrils $a_0 = 140$ nm, $d_0 = 5$ nm, initial aspect ratio of fibrils $\alpha_0 = a_0/d_0$, density of fibrillar material $\rho f = 3.1$ g/cm^3, number of fibrils in a unit cell $n_f = 6.8$, density of material at the initial time $\rho_0 = \rho_f\pi n_f/(4\alpha_0^2)$, surface diffusion coefficient $D_0 = 6.0 \cdot 10^{-20}$ m^2/s, activation energy of decomposition of hydroxide $E_D = 28 \pm 1$ kJ/mol, constant „free volume"

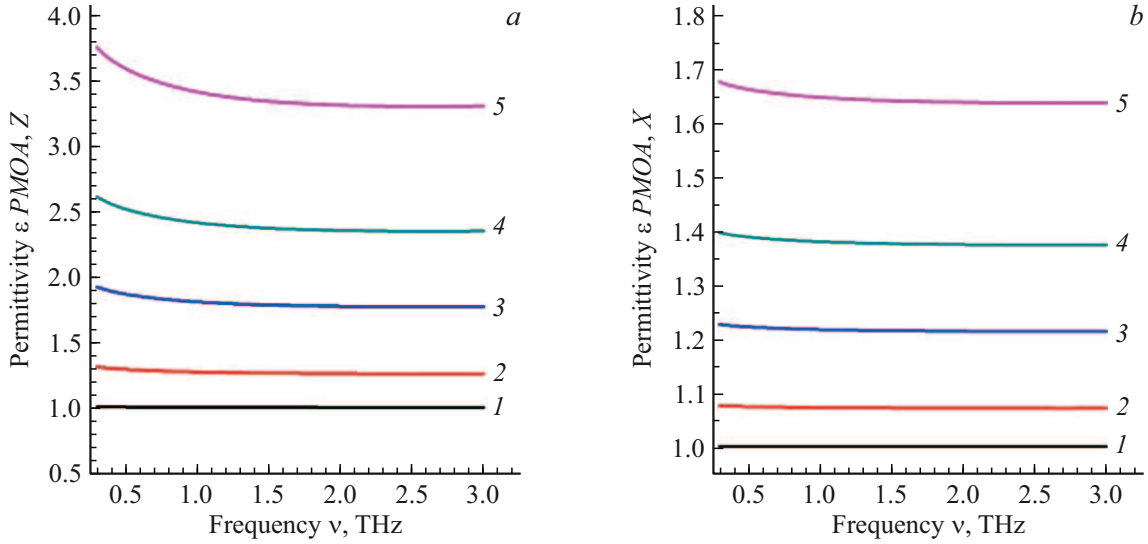


Figure 2. Dependence of the material part of the permittivity of AHPM materials on the frequency of ν THz radiation for the directions: (*a*) $\varepsilon_{\text{PMOA},Z}$ — along the growth axis *OZ*, and (*b*) $\varepsilon_{\text{PMOA},X}$ — in the transverse direction *OX* for nanostructures, annealed for 4 h at temperatures: *1* — 100°C; *2* — 1250°C; *3* — 1300°C; *4* — 1325°C; *5* — 1350°C.

$B_0 = 2.3 \cdot 10^{-2}\,\text{s}^{-1}$, activation energy of sintering process $E_b = 61$ kJ/mol, annealing time $t = 4\text{h} = 1.44 \cdot 10^4$ s, R — universal gas constant.

The switching between low-temperature ($T < 1000$°C) and high-temperature ($T > 1000$°C) annealing modes is formally modeled as follows:

$$\alpha = \alpha_D \left(\frac{1}{2} - \frac{1}{2}\tanh\left(\frac{T - T_0}{\Delta T}\right)\right) + \alpha_B \left(\frac{1}{2} + \frac{1}{2}\tanh\left(\frac{T - T_0}{\Delta T}\right)\right), \qquad (13)$$

where T is the annealing temperature, T_0 is the temperature in the vicinity of which the low-temperature regime is replaced by a high-temperature regime, ΔT is the characteristic temperature range in which both regimes coexist. We use $T_0 = 990$°C, $\Delta T = 120$°C in our calculations.

The volume fraction of aluminum oxide, structural and absorbed water, depending on the annealing temperature, is given by the formulas given in Ref. [4]. Thus, solving numerically the equation (8) at a given annealing temperature and time, we obtain $\varepsilon_{\text{PMOA},Z}$, as well as $\varepsilon_{\text{PMOA},X}$ and $\varepsilon_{\text{PMOA},Y}$.

Further development of the model will be associated with taking into account the heterogeneity of the fibrillar material, as well as the dispersion associated with the spatial orientation of the fibrils and clarifying its contribution to the optical anisotropy of the AHPM.

Results and discussion

Unless otherwise stated, our calculations assumed that the 3D structure of the AHPM samples has a texture — part of the fibrils is oriented along the axis *OZ*. Fig. 2 shows dependences of the real part of the dielectric constant $\varepsilon_{PMOA,Z}$ (*a*) and $\varepsilon_{PMOA,X}$ (*b*) on the temperature T (°C) of isochronous annealing 4 h and on the frequency of radiation ν (THz). At annealing temperatures $T \leq 900$°C, a relatively high porosity and a large geometric factor are maintained, therefore, the air environment occupies most of the free volume of the 3D structure. As the annealing temperature $T \geq 1000$°C increases, the amplitudes of both $\varepsilon_{PMOA,Z}$ and $\varepsilon_{PMOA,X}$ values increase and increase with temperature. This effect is associated with a change in the morphology of nanofibrils: the average aspect ratio decreases (the ratio of the length of the fibrill a to its diameter d), as a result, the bulk density of the AHPM material increases and the total porosity decreases — the contribution of aluminum oxides to the total dielectric constant begins to dominate.

The values of the imaginary parts of the dielectric permittivity ε_{PMOAZ} and ε_{PMOAX} also increase with temperature (Fig. 3), but with increasing frequency, the values of the imaginary parts show an inverse relationship. Similar dependences for the real (n') and imaginary (n'') parts of the refractive index $n = \sqrt{\varepsilon_{PMOAZ}}$ are shown in Figs. 4 and 5. The increase in absorption with decreasing frequency is due to the fact that the peak of bound water absorption is in the relatively low frequency range of 16 GHz. As follows from Fig. 6, the experimental data are in good agreement with the proposed model over a wide temperature range. A noticeable difference occurs in the range $1300\,\text{K} \leq T \leq 1600\,\text{K}$. Annealing in this temperature range causes a sequence of structural-phase transformations in AHPM fibrils: the initial amorphous hydrated pseudobemite $Al_2O_3 \cdot nH_2O$ [17], where $n \approx 4.6$, turns into γ-Al_2O_3, containing a small amount of structural water ($n < 0.1$), this process completes the transition to anhydrous phases: θ-Al_2O_3 and α-Al_2O_3 containing only water molecules

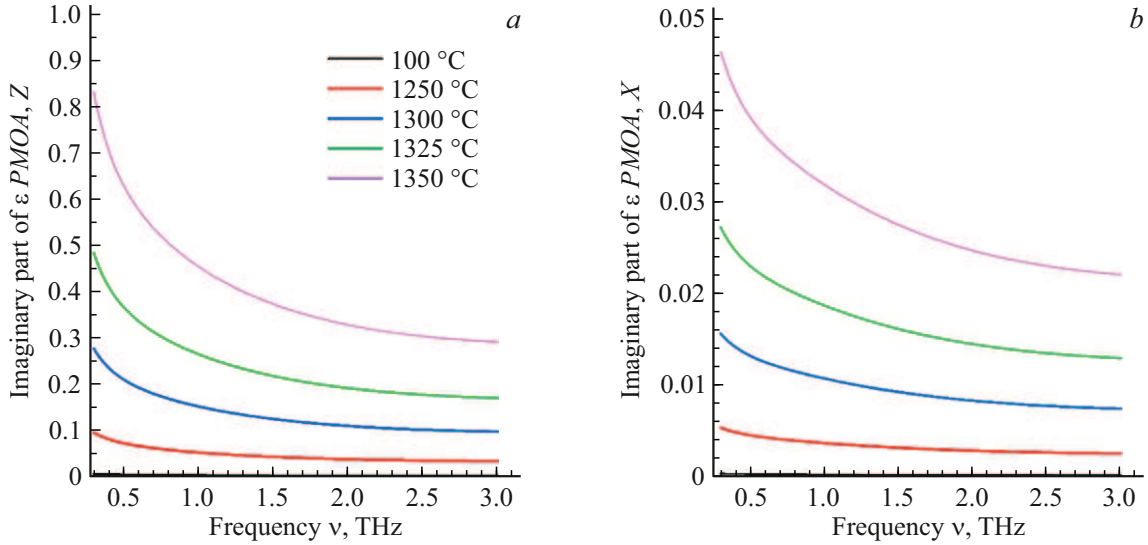


Figure 3. Dependence of the imaginary part of the refractive index $n = \sqrt{\varepsilon_{PMOA,Z}}$ on the frequency ν THz radiation for the directions: (*a*) n''_Z — in the direction along the OZ growth axis and (*b*) n''_X — in the transverse direction *OX* for nanostructures annealed for 4 h at temperatures: *1* — 100°C; *2* — 1250°C; *3* — 1300°C; *4* — 1325°C; *5* — 1350°C.

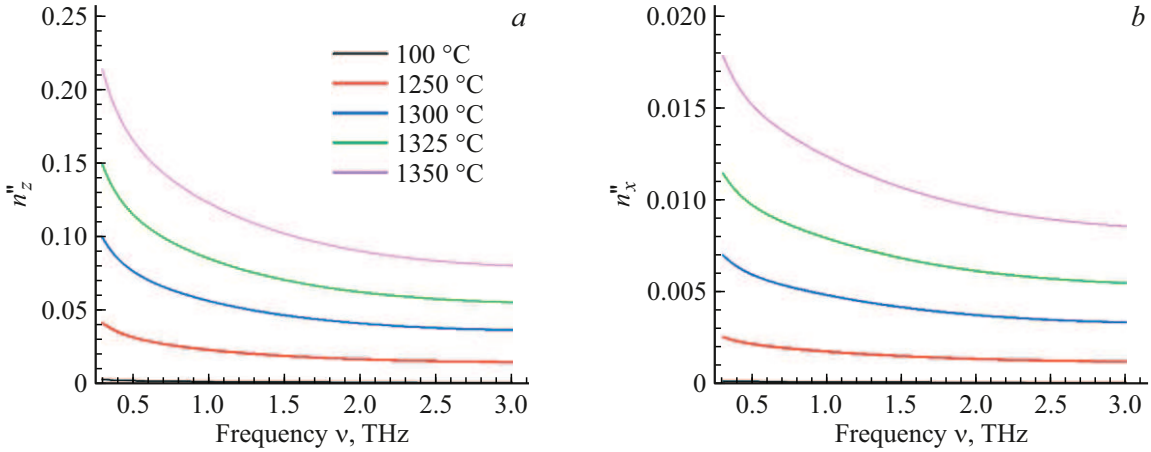


Figure 4. Dependence of the imaginary part of the refractive index $n = \sqrt{\varepsilon_{PMOA,Z}}$ on the frequency ν THz radiation for the directions: (*a*) n''_Z — in the direction along the OZ growth axis and (*b*) n''_X — in the transverse direction *OX* for nanostructures annealed for 4 h at temperatures: *1* — 100°C; *2* — 1250°C; *3* — 1300°C; *4* — 1325°C; *5* — 1350°C.

adsorbed on the surface. In the annealing process, the uniformity of the porous 3D nanomaterial increases, the dispersion decreases, and the total open porosity decreases to 30–25%.

It is important to note that the 3D nanostructure of AHPM materials has textural distortions, which is due to the peculiarities of the formation and 1D growth of nanofibrils, which are always directed strictly normally to the surface of the Me(Al) liquid metal alloy [4]. The estimates made within the framework of the proposed model confirmed the presence of anisotropy of optical properties: the ratio of the real parts $\varepsilon_{PMOA,Z}$ (measured along the direction of growth) and $\varepsilon_{PMOA,X}$ (measured in the perpendicular direction) can reach 2.28 (Fig. 2).

However, the fibrils in AHPM samples can be arranged in a more complex way. To account for these features, this model can be modified by formally introducing a volume fraction of f filaments oriented perpendicular to the axis *OZ*: $\leq f \leq 1$. In this case, the effective dielectric constant of the medium can be estimated as

$$\varepsilon_{ef,z} = (1-f)\varepsilon_{PMOA,z} + f\varepsilon_{PMOAx}),$$

$$\varepsilon_{ef,x} = f\varepsilon_{PMOA,z} + (1-f)\varepsilon_{PMOA,x}. \qquad (14)$$

The difference in the real parts of the refractive indices depending on the volume fraction of the f filaments is shown in Fig. 7. The difference in the real parts of the effective refractive indices may exceed one, which indicates a strong anisotropy in the distribution of nanofibrils. By

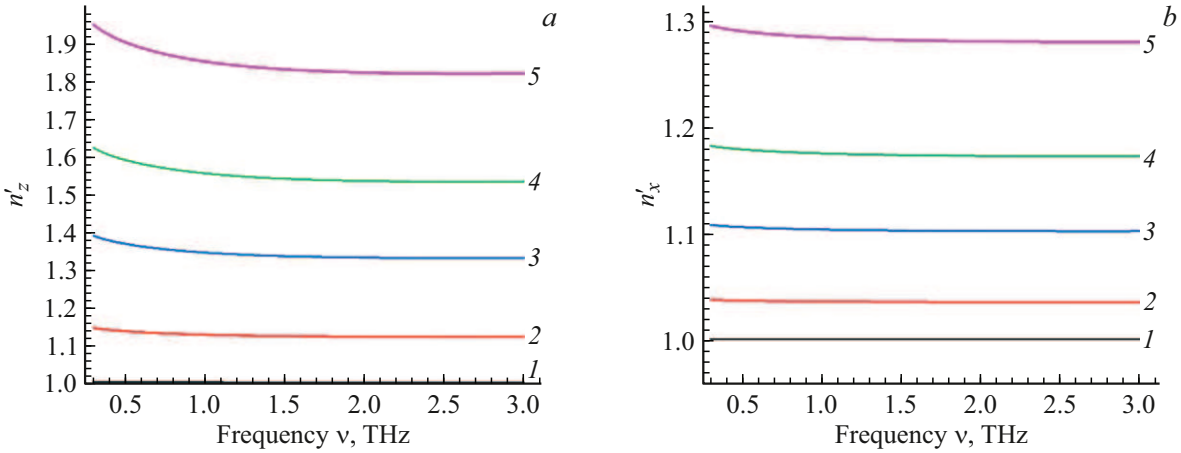


Figure 5. Dependence of the imaginary part of the refractive index $n = \sqrt{\varepsilon_{PMOA,Z}}$ on the frequency ν THz radiation for the directions: (*a*) n''_Z — in the direction along the OZ growth axis and (*a*) n'_Z — in the transverse direction OZ and (*b*) n'_x — in the transverse direction OX for nanostructures annealed for 4 h at temperatures: *1* — 100°C; *2* — 1250°C; *3* — 1300°C; *4* — 1325°C; *5* — 1350°C.

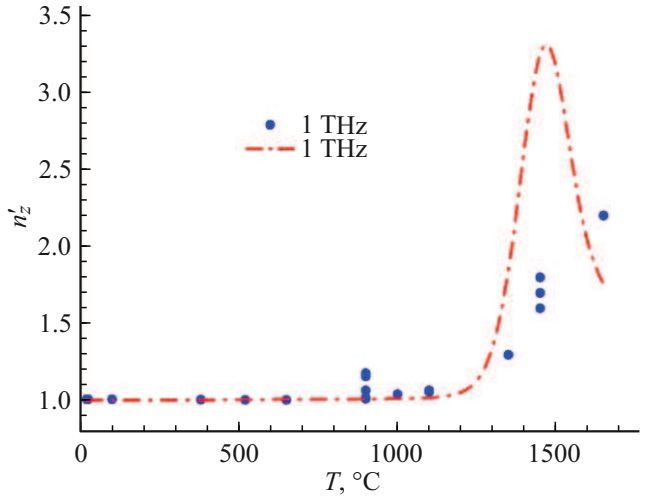


Figure 6. Comparison of experimental results of (•) measured at a frequency of 1 THz in the direction of AHPM growth (axis OZ) with theoretical estimates of the values of the real part of the dielectric constant n'_Z as a function of the annealing temperature T(°C).

measuring the difference in refractive indices for the OZ and OX directions, it is possible to judge the distribution of nanofibrils in the structure oriented along and across the growth direction of the AHPM.

The proposed model of the permittivity of AHPM for the THZ frequency range can be extended to the far and middle IR ranges, provided that the maximum sizes of aluminum oxide fibrils remain much smaller than the wavelength.

The development of laboratory nanotechnology based on AHPM opens up prospects for the creation of new functional 3D nanostructures and nanocomposites based on monolithic highly porous AHPM materials impregnated with metal, oxide or carbon nanoparticles. The dispersion properties of such materials will depend both on the total porosity of the AHPM and the content of impregnated nanoparticles, but also on the size and shape of the nanoparticles, their relative position, the average distance between the particles, and on the clustering of particles and the formation of extended structures along the surface of the fibrils. The formation of clusters and extended structures increases the probability of excitation of plasmons localized on metal particles. It is also possible to excite surface plasmon polaritons on structures consisting of ordered metal particles an clusters [13–16]. Under the conditions of plasmon resonance excitation, the electric field strength in the vicinity of metal particles and structures increases, which in turn increases the likelihood of nonlinear optical

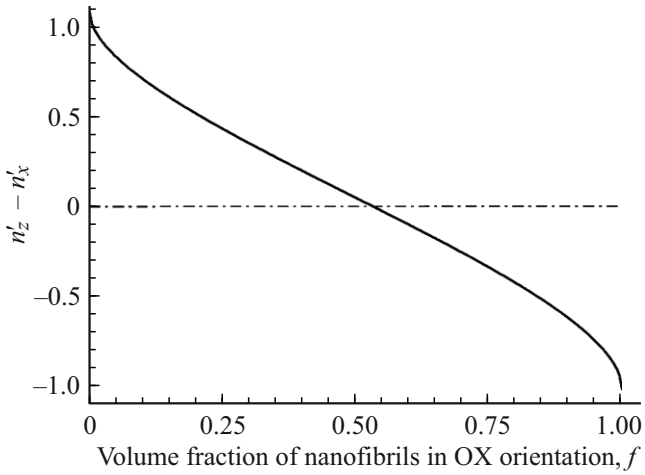


Figure 7. Estimation of the difference between the real part of the effective refractive n'_Z and $'_X$ for directions along the direction of AHPM growth (axis OZ) and across (axis OX) depending on the change in the volume fraction of nanofibrils oriented along the axis OZ. Calculations were performed for a AHPM sample annealed with 4 h at a temperature of $T = 1300$°C for a frequency of $\nu = 1$ THz.

processes, but in this case, in order to correctly describe the optical properties of the material, it will be necessary to abandon the Maxwell-Garnett relation, replacing it, for example, with the Bruggeman formula.

The proposed model is an initial stage and suggests its further development in search of a more general solution to the physical problem of quantifying the interaction of THz-band radiation with metamaterials based on porous 3D oxide nanostructures and nanocomposites with a chemically modified surface [5] or impregnated with Ag, Au nanoparticles. Such nanocomposites have already been synthesized, and their physical properties are currently being studied.

Conclusions

Based on the model of the structural evolution of AHPM materials [4], a physical model of the effective dielectric constant of porous 3D oxide nanostructures has been developed based on the Bruggeman formula and the Maxwell–Garnett approximation, taking into account the depolarization effects associated with the shape of nanofibrils. The proposed model opens up the prospect of further development of models of the dielectric permittivity of nanocomposite metamaterials based on porous 3D oxide nanostructures with a chemically modified surface or impregnated with metal nanoparticles.

Funding

This work uses the results of experimental studies of 3D nanostructures of aluminum oxy-hydroxides by pulsed THz spectroscopy, performed in accordance with the work plan under the RFBR grant 22-23-01011, and theoretical models developed during the work under the RFBR grant 18-02-00528.

Conflict of interest

The authors declare that they have no conflict of interest.

References

[1] S.M. Korobkov, K.P. Birin, A.N. Khodan et al. Int. J. Mol. Sci., **24** (15), 12165 (2023). DOI: 10.3390/ijms241512165
[2] A.V. Svetlakova, M.S. Mendez, E.S. Tuchin et al. Opt. Spectrosc., **129** (8), 846–850 (2021). DOI: 10.1134/S0030400X21060175
[3] K.I. Zaytsev, I.N. Dolganova, N.V. Chernomyrdin et al. J. Opt., **22** (1), 013001 (2020). DOI: 10.1088/2040-8986/ab4dc3
[4] A. Khodan, T.H.N. Nguyen, M. Esaulkov et al. J. Nanopart. Res., **20**, 194–201 (2018). DOI: 10.1007/s11051-018-4285-4
[5] A. Khodan, A. Kanaev, M. Esaulkov et al. Nanomaterials, **12** (20), 3591–3603 (2022). DOI: 10.3390/nano12203591
[6] A.P. Vinogradov. *Elektrodinamika kompozitnyh materialov*, pod red. B.Z. Kacenelenbauma (Editorial URSS, M., 2001). p. 208 (in Russian).
[7] P.H. Bolivar, M. Brucherseifer, J.G. Rivas et al. IEEE Trans. Microw. Theory Tech., **51** (4), 1062–1066 (2003). DOI: 10.1109/TMTT.2003.809693
[8] A.A. Angeluts, A.V. Balakin, M.G. Evdokimov et al. Quantum Electron., **44** (7), 614–632 (2014). DOI: 10.1070/QE2014v044n07ABEH015565
[9] P. Lunkenheimer, S. Emmert, R. Gulich et al. Phys. Rev. E, **96** 062607 (2017). DOI: 10.1103/PhysRevE.96.062607
[10] N. Penkov, V. Yashin, E. Fesenko, A. Manokhin et al. Appl. Spectr., **72** (2) 257–267 (2018). DOI: 10.1177/0003702817735551
[11] L.A. Apresyan, D.V. Vlasov, D.A. Zadorin, V.I. Krasovsky. ZhTF, **87** (1) 10-17 (2017) (in Russian). https://journals.ioffe.ru/articles/viewPDF/44011
[12] D.A.G. Bruggeman. Annalen der Physik, **416** (75), 636–664 (1935). DOI: 10.1002/andp.19354160705
[13] L.A. Golovan, V.Yu. Timoshenko, P.K. Kashkarov. Physics-Uspekhi, **50** (6), 595–612 (2007). DOI: 10.1070/PU2007v050n06ABEH006257
[14] O.A. Smolyanskaya, N.V. Chernomyrdin, A.A. Konovko et al. Prog. Quantum Electron., **62**, 1–77 (2018). DOI: 10.1016/j.pquantelec.2018.10.001
[15] V.V. Klimov. *Nanoplazmonika*, izd. 2, ispr. (Fizmatlit, M., 2010). p. 480. ISBN 978-5-9221-1205-5 (in Russian).
[16] E.S. Andrianov, A.P. Vinogradov, A.V. Dorofeenko, A.A. Puhov, A.A. Zyablovskij, A.A. Lisyanskij. *Kvantovaya nanoplazmonika*. Uchebnoe posobie (Izdatel'skij dom .Intellekt., Dolgoprudnyj, 2015). p. 368 (in Russian). ISBN 978-5-91-559203-1
[17] S. Iijimaa, T. Yumura, Zh. Liu. PNAS, **113** (42), 11759–11764 (2016). DOI: 10.1073/pnas.1614059113

Translated by A.Akhtyamov